Effects of Suction and Blowing on Flow and Heat Transfer Between Two Rotating Spheres With Time-Dependent Angular Velocities

Omid Mahian
Graduate Student

Asgahr B. Rahimi[1]
Professor
e-mail: rahimiab@yahoo.com

Faculty of Engineering,
Ferdowsi University of Mashhad,
P.O. Box No. 91775-1111,
Mashhad, Iran

Ali Jabari Moghadam
Assistant Professor
Shahrood University of Technology,
P.O. Box 316,
Shahrood, Iran

The effect of suction and blowing in the study of flow and heat transfer of a viscous incompressible fluid between two vertically eccentric rotating spheres is presented when the spheres are maintained at different temperatures and rotating about a common axis while the angular velocities of the spheres are arbitrary functions of time. The resulting flow pattern, temperature distribution, and heat transfer characteristics are presented for the various cases including exponential and sinusoidal angular velocities. These presentations are for various values of the flow parameters including rotational Reynolds number Re, and the blowing/suction Reynolds number Re_w. The effects of transpiration and eccentricity on viscous torques at the inner and outer spheres are studied, too. As the eccentricity increases and the gap between the spheres decreases the viscous torque remains nearly unchanged. Results for special case of concentric spheres are obtained by letting eccentricity tend to zero. [DOI: 10.1115/1.4003604]

Keywords: flow and heat transfer, rotating spheres, time-dependent angular velocities, suction and blowing

1 Introduction

The flow and heat transfer in an annulus between two spheres have been studied in various cases by many researchers. Such studies can be classified into two main groups. In the first group, there is neither suction nor blowing at the spherical walls. Such containers are used in engineering designs such as centrifuges and fluid gyroscopes and also are important in geophysics. Available theoretical works concerning such problems are primarily of a boundary-layer or singular-perturbation character considered by Howarth [1], Proudman [2], Lord and Bowden [3], Fox [4], Greenspan [5], Carrier [6], and Stewartson [7]. The first numerical study of time-dependent viscous flow between two rotating spheres has been presented by Pearson [8] in which case one or both of the spheres is given an impulsive change in angular velocity starting from a state of either rest or uniform rotation. Munson and Joseph [9] considered the case of steady motion of a viscous fluid between concentric rotating spheres using perturbation techniques for small values of Reynolds number and a Legendre polynomial expansion for larger values of Reynolds numbers. Thermal convection in rotating spherical annuli has been considered by Douglass et al. [10]. A study of viscous flow in oscillatory spherical annuli has been done by Munson and Douglass [11] in which a perturbation solution valid for slow oscillation rates is presented and compared with experimental results. Another interesting work is the study of the axially symmetric motion of an incompressible viscous fluid between two concentric rotating spheres done by Gagliardi et al. [12], and also the study by Yang et al. [13] and the finite element study by Ni and Nigro [14]. These problems include cases where one or both spheres rotate with prescribed constant angular velocities and the case in which one sphere rotates due to the action of an applied constant or impulsive torque. Recently, a numerical study of flow and heat transfer between two rotating spheres has been done by Jabari Moghadam and Rahimi [15] in which the fluid contained between two vertically eccentric spheres maintained at different temperatures and rotating about a common axis with different angular velocities when the angular velocities are arbitrary functions of time. Jabari Moghadam and Rahimi [16] also studied the similarity solution for spheres rotating with constant angular velocity.

In the second group, the effects of transpiration on flow in an annulus between two spheres have been investigated. The study of flow in a spherical annulus along with transpiration is used in many practical applications, such as rotary machines and spherical heat exchangers and in the design of spherical fluid storage systems. In these applications transpiration is used to regulate the rate of heat transfer.

The effects of transpiration on free convection in an annulus between two stationary concentric porous spheres have been considered by Gulwadi and Elkouh [17]. Gulwadi et al. [18] studied the laminar flow in an annulus between rotating porous spheres and with injection and suction at spherical walls. They used a perturbation technique to solve the steady-state Navier–Stokes equations of motion and also used a finite-difference method to validate their analytical results. Their results are valid for small values of the rotational Reynolds number and an injection/suction Reynolds number, and the heat transfer has not been considered. A review of literature reveals that there are no studies on the transient motion and the heat transfer between two rotating spheres with uniform transpiration.

In the present study, a numerical solution of unsteady momentum and energy equations is presented for the general case of viscous flow between two vertically eccentric rotating spheres maintained at different temperatures along with suction and blowing at their boundaries, which are rotating with time-dependent angular velocities. Results for some example functions including

[1]Corresponding author.

Contributed by the Heat Transfer Division of ASME for publication in the JOURNAL OF HEAT TRANSFER. Manuscript received November 8, 2009; final manuscript received February 6, 2011; published online April 1, 2011. Assoc. Editor: Terrence W. Simon.

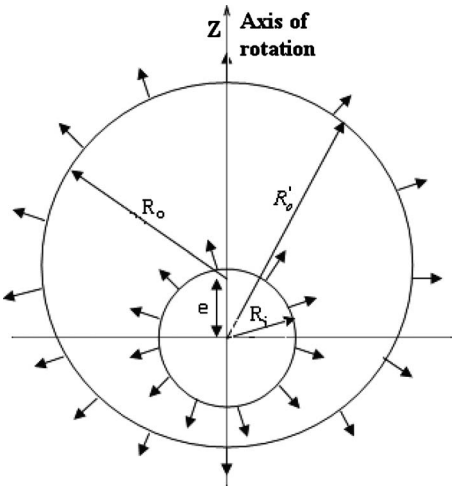

Fig. 1 Geometry of eccentric rotating spheres

exponential and sinusoidal angular velocities and various blowing/suction Reynolds numbers Re_w are presented when the outer sphere initially starts rotating with a constant angular velocity and the inner sphere starts rotating with a prescribed time-dependent function. Results for the special case of concentric spheres are obtained by letting eccentricity tend to zero.

2 Problem Formulation

The geometry of the spherical annulus considered is indicated in Fig. 1. The vertical eccentricity of the outer sphere is measured by the distance e. If the outer sphere is placed above the central position, e has a positive value; otherwise it is negative. The origin of the spherical coordinate system is the inner sphere center and the characteristic radius of the outer sphere R_o' is a function of θ. A Newtonian, viscous, incompressible fluid fills the gap between the inner and outer spheres, which are of radii R_i and R_o and with constant surface temperatures T_i and T_o and rotate about a common axis with angular velocities Ω_i and Ω_o, respectively. The components of velocity in r, θ, and ϕ directions are v_r, v_ϕ, and v_ϕ, respectively. These velocity components for incompressible flow and in the meridian plane satisfy the continuity equation and are related to the stream function ψ and angular momentum function Ω in the following manner:

$$v_r = \frac{\psi_\theta}{r^2 \sin\theta}, \quad v_\theta = \frac{-\psi_r}{r \sin\theta}, \quad v_\phi = \frac{\Omega}{r \sin\theta} \tag{1}$$

The blowing/suction Reynolds number is defined as

$$\mathrm{Re}_w = \frac{v_{r_o} r_o}{\nu} \tag{2}$$

in which v_{r_o} and r_o are radial velocity and radius reference values, respectively. The blowing/suction Reynolds number Re_w is positive for blowing at the inner sphere and negative for suction. Since the flow is assumed to be independent of the longitude ϕ, the nondimensional Navier–Stokes equations and energy equation can be written in terms of the stream function and the angular velocity function as follows:

$$\frac{\partial \Omega}{\partial t} + \frac{\psi_\theta \Omega_r - \psi_r \Omega_\theta}{r^2 \sin\theta} = \frac{1}{(\mathrm{Re})} D^2 \Omega \tag{3}$$

$$\frac{\partial}{\partial t}(D^2\psi) + \frac{2\Omega}{r^3 \sin^2\theta}[\Omega_r r \cos\theta - \Omega_\theta \sin\theta] - \frac{1}{r^2 \sin\theta}[\psi_r (D^2\psi)_\theta - \psi_\theta (D^2\psi)_r] + \frac{2D^2\psi}{r^3 \sin^2\theta}[\psi_r r \cos\theta - \psi_\theta \sin\theta] = \frac{1}{(\mathrm{Re})} D^4\psi \tag{4}$$

$$\frac{\partial T}{\partial t} + v_r \frac{\partial T}{\partial r} + \frac{v_\theta}{r}\frac{\partial T}{\partial \theta} = \frac{1}{(\mathrm{Pe})}\left[\frac{\partial^2 T}{\partial r^2} + \frac{2}{r}\frac{\partial T}{\partial r} + \frac{1}{r^2}\frac{\partial^2 T}{\partial \theta^2} + \frac{\cot\theta}{r^2}\frac{\partial T}{\partial \theta}\right] + (Ek)\left\{2\left[\left(\frac{\partial v_r}{\partial r}\right)^2 + \left(\frac{1}{r}\frac{\partial v_\theta}{\partial \theta} + \frac{v_r}{r}\right)^2 + \left(\frac{v_r}{r} + \frac{v_\theta}{r}\cot\theta\right)^2\right] + \left[r\frac{\partial}{\partial r}\left(\frac{v_\theta}{r}\right) + \frac{1}{r}\frac{\partial v_r}{\partial \theta}\right]^2 + \left[\frac{\sin\theta}{r}\frac{\partial}{\partial \theta}\left(\frac{v_\phi}{\sin\theta}\right)\right]^2 + \left[r\frac{\partial}{\partial r}\left(\frac{v_\phi}{r}\right)\right]^2\right\} \tag{5}$$

in which the nondimensional quantities Reynolds number (Re), Prandtl number (Pr), Peclet number (Pe), and Eckert number (Ek) are defined as

$$\mathrm{Re} = \frac{\omega_o r_o^2}{\nu}, \quad \mathrm{Pr} = \nu/\alpha, \quad \mathrm{Pe} = \mathrm{Re}\ \mathrm{Pr} = \frac{\omega_o r_o^2}{\alpha}, \quad \mathrm{Ek} = \frac{\nu \omega_o}{c_p (T_o - T_i)} \tag{6}$$

The following nondimensional parameters have been used in the above equations and then the asterisks have been omitted:

$$t^* = t\omega_o, \quad r^* = \frac{r}{r_o}, \quad \psi^* = \frac{\psi}{r_o^3 \omega_o}, \quad \Omega^* = \frac{\Omega}{r_o^2 \omega_o}, \quad T^* = \frac{T - T_i}{T_o - T_i} \tag{7}$$

in which ω_o is reference value. The nondimensional boundary and initial conditions for the above governing equations are

For $t < 0$

$$\begin{cases} \psi = 0 \\ \Omega = 0 \\ T = 0 \end{cases} \quad \text{everywhere}$$

For $t \geq 0$

$$\theta = 0 \rightarrow \{\psi_r = 0, \psi_\theta = 0, \Omega = 0\}, \frac{\partial T}{\partial \theta} = 0$$

$$\theta = \pi \rightarrow \{\psi_r = 0, \psi_\theta = 0, \Omega = 0\}, \frac{\partial T}{\partial \theta} = 0$$

$$r = R_i/R_o \rightarrow \left\{ \psi_\theta = \frac{\mathrm{Re}_w}{\mathrm{Re}} \sin\theta \ , \psi_r = 0, \Omega = \frac{\Omega_i R_i^2}{\omega_o R_o^2} \sin^2\theta, T = 0 \right. \tag{8}$$

$$r = R_o'/R_o = e\cos\theta + \sqrt{(1 - e^2 \sin^2\theta)} \rightarrow \left\{ \psi_\theta = \frac{\mathrm{Re}_w \cdot R_o'^2}{\mathrm{Re} \cdot R_o^2} \sin\theta, \psi_r = 0, \Omega = \frac{\Omega_o R_o'^2}{\omega_o R_o^2} \sin^2\theta, T = 1 \right.$$

where

$$D^2 \equiv \frac{\partial^2}{\partial r^2} + \frac{1}{r^2}\frac{\partial^2}{\partial \theta^2} - \frac{\cot\theta}{r^2}\frac{\partial}{\partial \theta}$$

These governing equations along with the related boundary and initial conditions are solved numerically in Sec. 3.

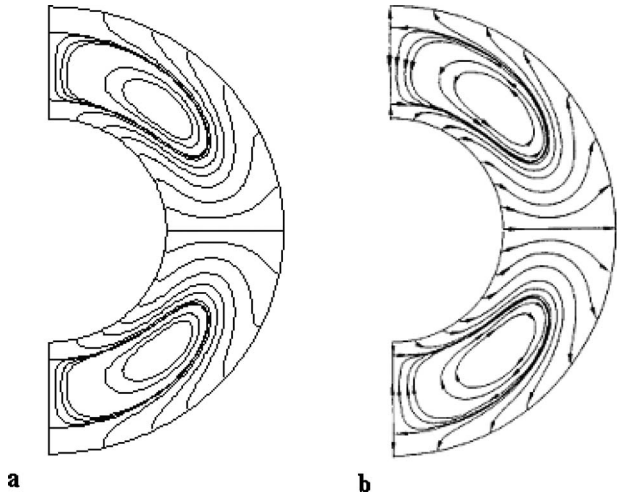

Fig. 2 Contours of ψ for Re=20, Re_w=0.5, Ω_{oi}=0, and e=0

3 Computational Procedure

The two equations governing the fluid motion show that each is describing the behavior of one of the dependent variables Ω and ψ. On the other hand, these two equations are coupled only through nonlinear terms. To solve the problem, the momentum equations were discretized by the finite-difference method and implicit scheme. Because of the known velocity field, the energy equation is linear and is solved keeping all its terms. In each time step $(n+1)$, the value of the dependent variables are guessed from their values at previous time steps (n), $(n-1)$, and $(n-2)$ and after using them in difference equations and repeating it until the desired convergence will lead to the corrected values at this time step. This procedure is applied for the next time step.

The flow field considered is covered with a regular mesh. To solve the system of linear difference equations, a tridiagonal method algorithm is used in both directions r and θ [19]. Direct substitution of previous values of dependent variables by new calculated values can cause calculation unstability in general. To overcome this problem, a weighting procedure is used in which the optimum weighting factor depends on Reynolds number. The mesh size used in the numerical solution for the equator of the circle is a uniform 40×20, 60×30, 80×40, and 100×50 (θ-direction $\times r$-direction, respectively) with the ratio of $R_{out}/R_{in}=2$, which all of them show that the problem is independent of mesh size, but on one hand by noting the calculation time and on the other hand since a finer mesh size is better we choose the 80×40 mesh size. In this work, the sphere angular velocity has been considered a function of time and to apply this time function to the program, an average value at the beginning of each time step has been calculated and used for the sphere angular velocity function. Therefore, for each considered time step, the sphere velocity is defined and sectionally continues. To verify the validity of the numerical procedure used in this work, a comparison with Ref. [18] has been done, which shows very good agreement, as is shown in Fig. 2. Also comparison with Ref. [15] is conducted to examine the effects of transpiration on flow and heat transfer for various values of blowing/suction Reynolds number Re_w.

4 Presentation of Results

The flow pattern in the meridian plane for Re=20 and Re_w =0.5 is shown in Fig. 2(*a*). Comparison between the present work and Ref. [18], Fig. 2(*b*), shows very good agreement. In this case, the outer sphere is stationary and the inner sphere rotates with constant angular velocity ($\Omega_{oi}=\Omega_o/\Omega_i=0$). Here, therefore, the characteristics of the inner sphere including v_{R_i}, Ω_i, and R_i are considered as reference values. Since the blowing/suction Reynolds number Re_w is low in comparison with the rotational Reynolds number Re then as can be seen in Fig. 2 the eddies created by the centrifugal effect generated by the rotation of the inner sphere are confined within regions near the poles and cause two stagnation points on the streamlines at the poles (θ=0 deg and θ=180 deg). As will be mentioned in section 5, these eddies are preventive means for the heat transfer.

The contours of ψ and T for Re=1000, Re_w=5, Pr=1, $\Omega_{io}=-\exp(1-t)$, e=0.1, and Ek=0 are shown in Figs. 3 and 4, respectively. As can be seen from Fig. 3(*a*), at the beginning the eddies are created in the upper hemisphere and near the pole (θ =0 deg), so that two stagnation points exist on the pole. Note that due to eccentricity the flow field is asymmetric with respect to the equator plane and on the other hand because of more Coriolis forces in the lower hemisphere the eddies are eliminated near the pole (θ=180 deg). Also it is seen from this figure that by decreasing the eccentricity, the size of the eddies in the upper hemisphere decreases while as the eccentricity tends to zero, the eddies will be formed in the lower sphere, too. Then in the concentric case, four stagnation points exist on the poles. Also, the effects of blowing on vortices can be obtained in comparison with Ref. [15]. It is

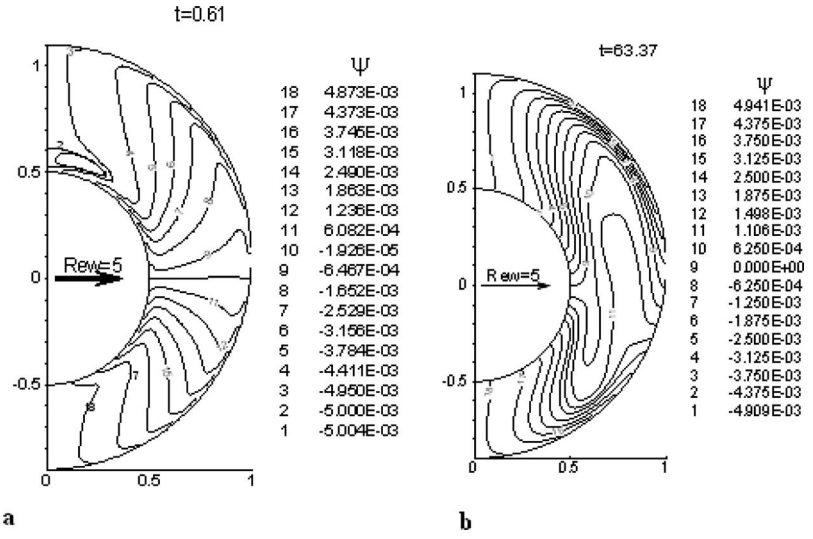

Fig. 3 Contours of ψ for Re=1000, Re_w=5, $\Omega_{io}=-\exp(1-t)$, and e=0.1

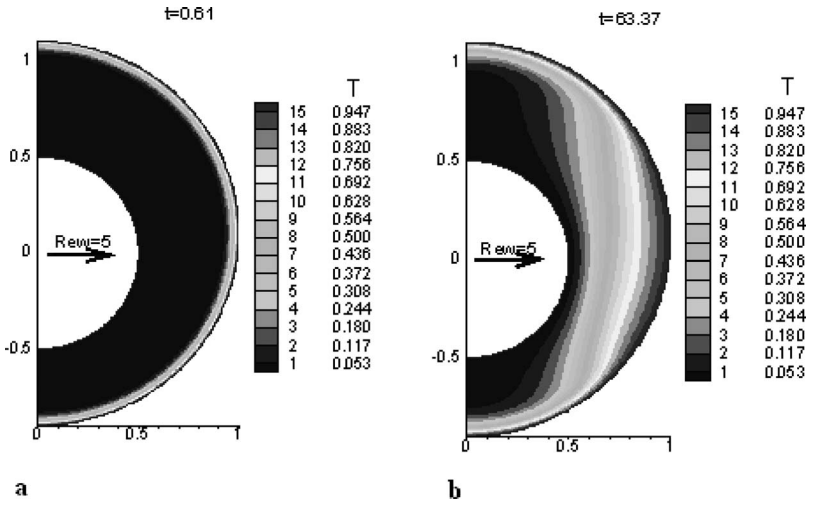

Fig. 4 Contours of T for Re=1000, Re_w=5, Pr=1, $\Omega_{io}=-\exp(1-t)$, and e=0.1

observed that the blowing removes all of the vortices in the fourth quadrant and also the vortices near the outer sphere in the first quadrant. As time advances, the streamlines in the vicinity of the equator become irregular while in the vicinity of the poles, the streamlines are smoother, Fig. 3(*b*). At this time, there is no eddy in the vicinity of the poles. Now, considering the contours of (ψ), the distribution of temperature (T) can be described better. From Fig. 4(*a*), it is observed that at the beginning, the distribution of temperature in the annulus space is nearly uniform and the eddies in the upper hemisphere do not affect the temperature field. As time passes, the blowing effect covers the entire temperature field so that it grows less than the case $Re_w=0$; but, because of smoother streamlines in the vicinity of the poles, the cold flow from the inner sphere toward the outer sphere transfers more heat than the regions far from the poles.

Figures 5–12 present the ψ and T contours for various blowing/suction Reynolds numbers Re_w for the same conditions as in Figs. 3 and 4. By comparing Figs. 5 and 3 , it can be seen that an increase in blowing at the beginning, the eddies in the upper hemisphere are eliminated and the streamlines in the initial and final times are smoother. Also, because of more blowing, the vortices do not penetrate from the first quadrant into the fourth quadrant by the final time. Figure 6(*b*) in comparison with Fig. 4(*b*) shows less penetration of the temperature field in the final time due to an increase in blowing rate.

Figure 7 shows the effect of increase in blowing on contours of ψ in which increasing Re_w (approximately larger than $Re_w \approx 25$) induces fully straight streamlines or, in other words, the blowing overcomes rotational motion in the annulus space completely. Contours of T for $Re_w=20$ are shown in Fig. 8. Note that at the beginning the effect of blowing on temperature field is not much visible in various Re_w.

Figure 9 shows the streamlines for suction case with $Re_w=-5$. As is shown, in this case contrary to the case $Re_w=5$, eddies are created near the outer sphere in the upper hemisphere. The distance between the stagnation points in the first quadrant increases with time and also eddies are created in the fourth quadrant but with a lesser size. Effects of eddies, which can be seen in Fig. 9(*b*), on the diffusion of heat from the outer sphere into the field can be seen also in Fig. 10(*b*). As can be seen in this case, in regions near the poles the heat diffusion is less than the regions far from the poles. In these regions the eddies are preventing the heat convection, then near the poles, conduction is the dominant

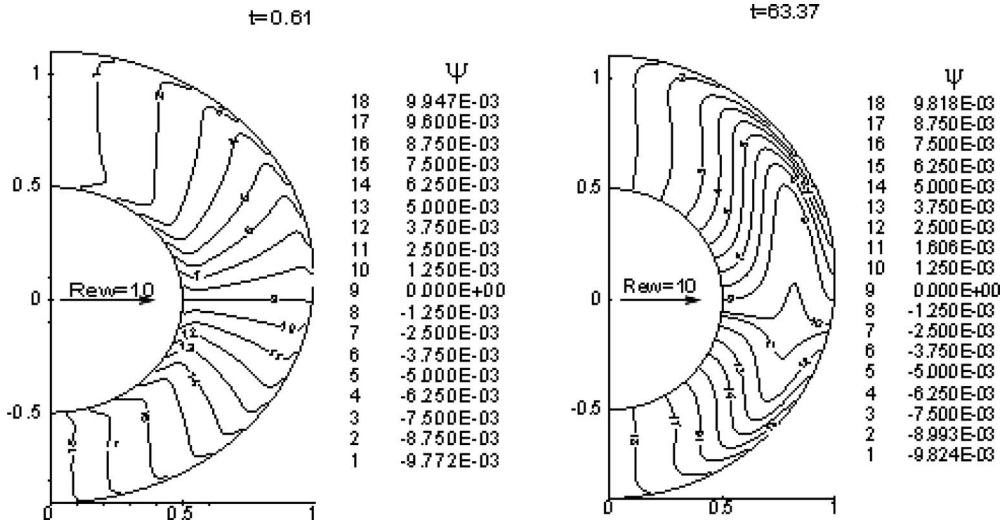

Fig. 5 Contours of ψ for Re=1000, Re_w=10, $\Omega_{io}=-\exp(1-t)$, and e=0.1

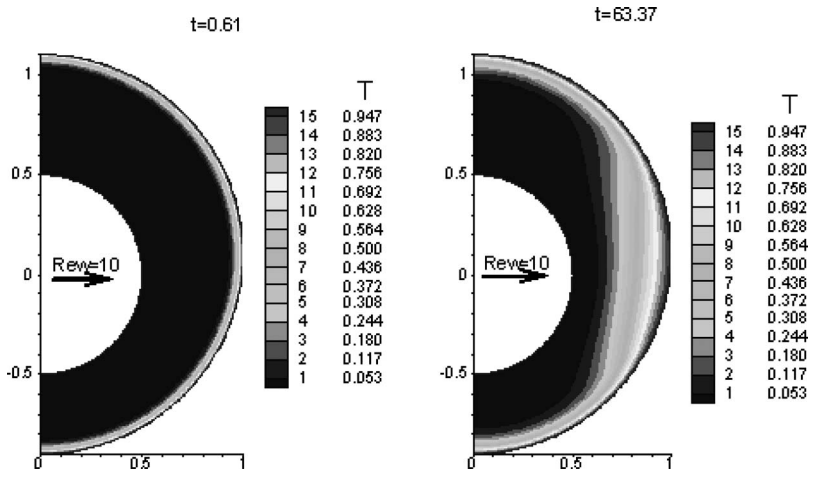

Fig. 6 Contours of T for Re=1000, Re_w=10, Pr=1, $\Omega_{io}=-\exp(1-t)$, and e=0.1

mechanism of heat diffusion. Also note that the diffusion of heat is more visible in the lower hemisphere.

With an increase in suction, it is observed that at the beginning, eddies are eliminated, as is seen in Fig. 11(*a*) compared with Fig. 9(*a*). Also Fig. 11(*b*) shows that the streamlines penetrate with time from the first quadrant into the fourth quadrant. As can be seen in Fig. 12(*b*), the effect of suction on the diffusion of heat from the outer sphere into the field is considerable. Note that the factors such as Prandtl number (Pr) and blowing/suction Reynolds number have important roles in the diffusion of heat, so that an increase in Prandtl number or blowing/suction Reynolds number decreases the heat diffusion of the outer sphere into the field.

Figures 13 and 14 have been presented for inner angular velocity $\Omega_{io}=2\sin(\pi t/2)$ for Re=1000, Re_w=5, Pr=10, e=0.1, and

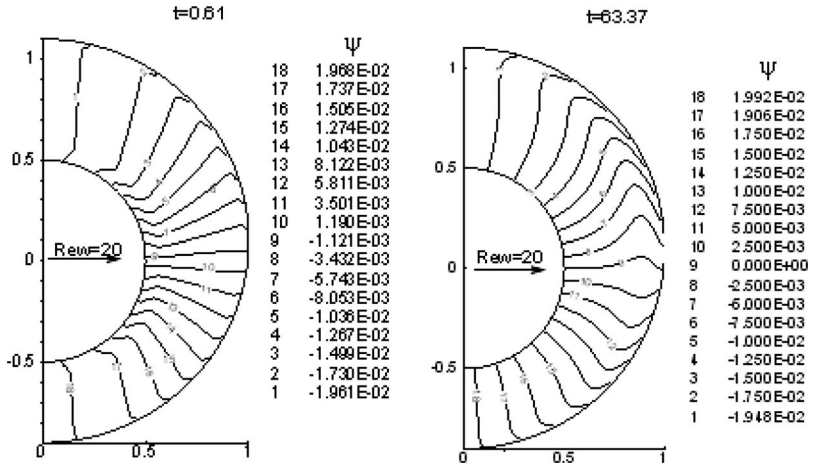

Fig. 7 Contours of ψ for Re=1000, Re_w=20, $\Omega_{io}=-\exp(1-t)$, and e=0.1

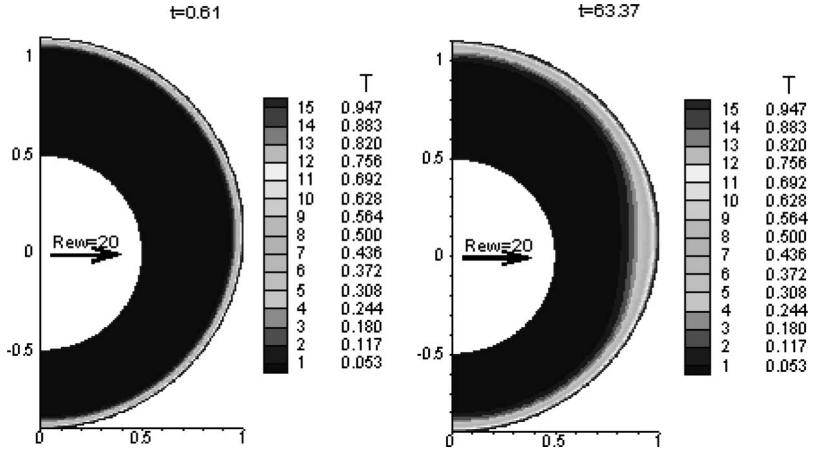

Fig. 8 Contours of T for Re=1000, Re_w=20, Pr=1, $\Omega_{io}=-\exp(1-t)$, and e=0.1

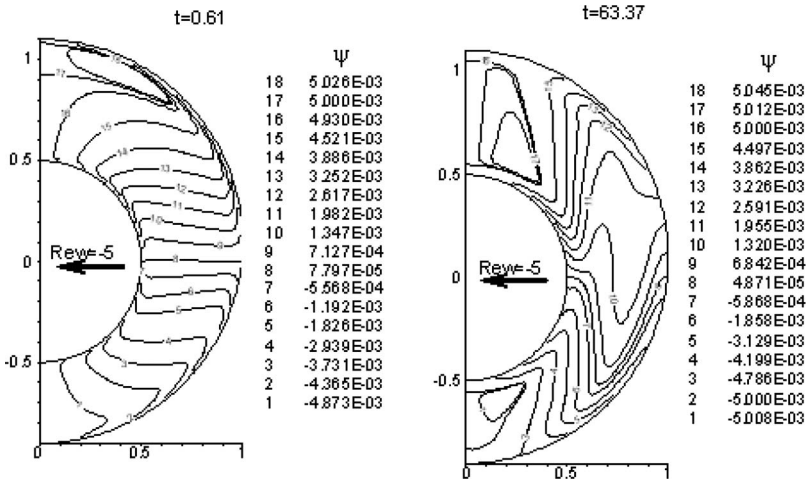

Fig. 9 Contours of ψ for Re=1000, $Re_w=-5$, $\Omega_{io}=-\exp(1-t)$, and $e=0.1$

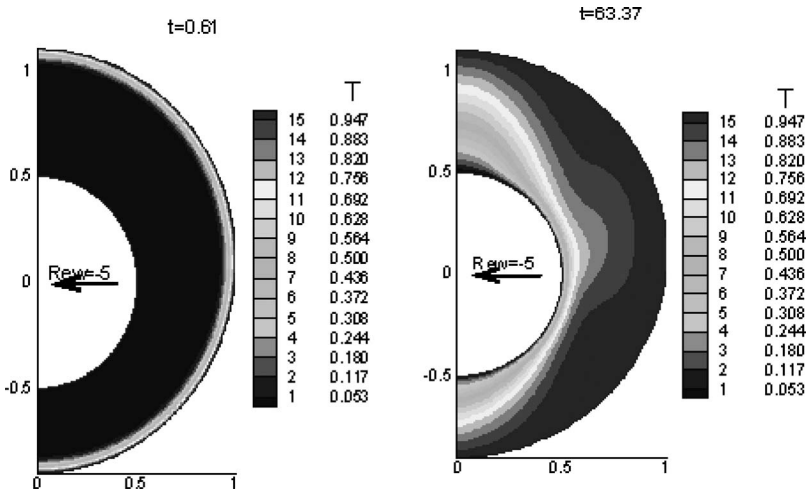

Fig. 10 Contours of T for Re=1000, $Re_w=-5$, Pr=1, $\Omega_{io}=-\exp(1-t)$, and $e=0.1$

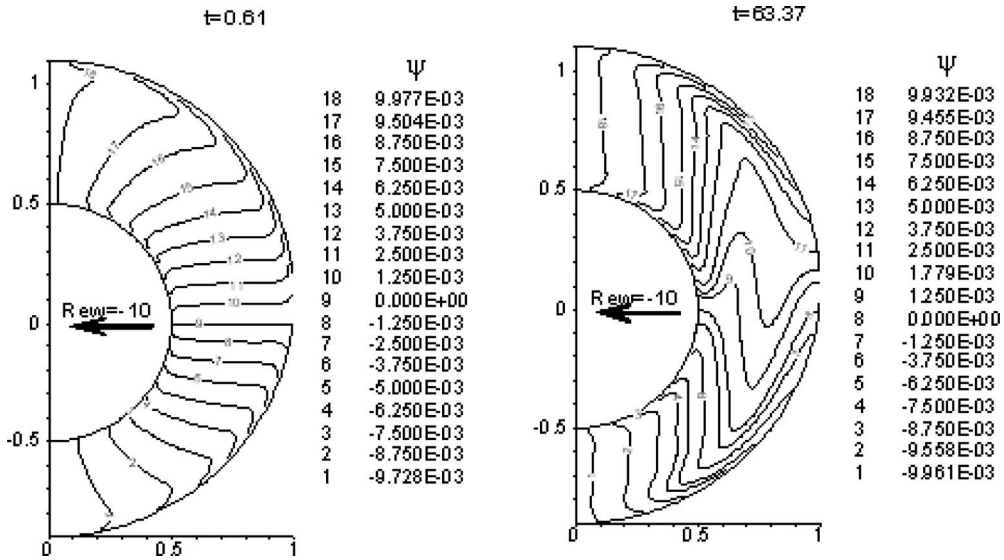

Fig. 11 Contours of ψ for Re=1000, $Re_w=-10$, $\Omega_{io}=-\exp(1-t)$, and $e=0.1$

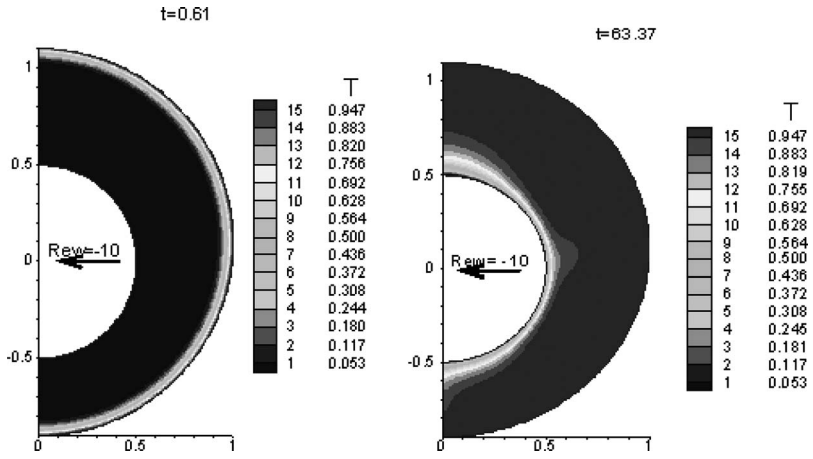

Fig. 12 Contours of T for Re=1000, $Re_w=-10$, Pr=1, $\Omega_{io}=-\exp(1-t)$, and $e=0.1$

Ek=0 and in two consecutive periods (second and third) for the sinusoidal function. As can be seen in Fig. 13(*a*) eddies are created in the vicinity of the poles as well as the equator in both quadrants and because of larger Coriolis forces, the sizes of eddies in the lower hemisphere are smaller. Figure 13(*b*) shows that the sizes of eddies in the vicinity of the poles have been increased, especially at the upper pole. But change in the size and position of the eddies in the vicinity of the equator is not considerable. Also

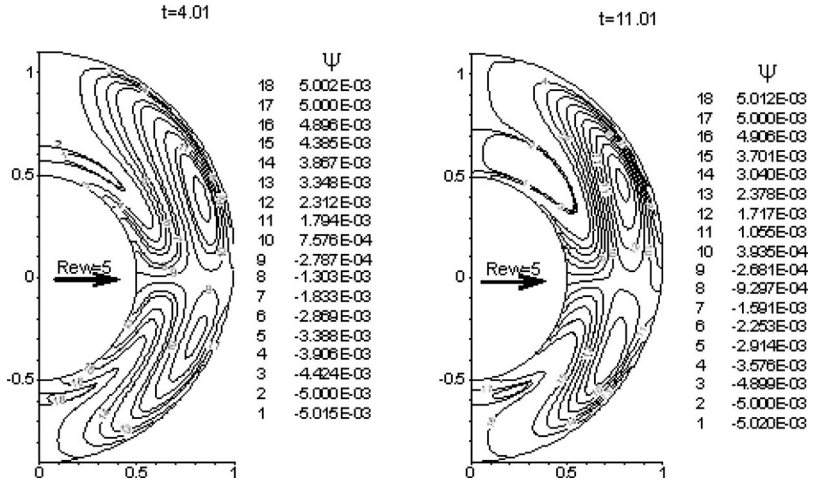

Fig. 13 Contours of ψ for Re=1000, $Re_w=5$, $\Omega_{io}=2\sin(\pi t/2)$, and $e=0.1$

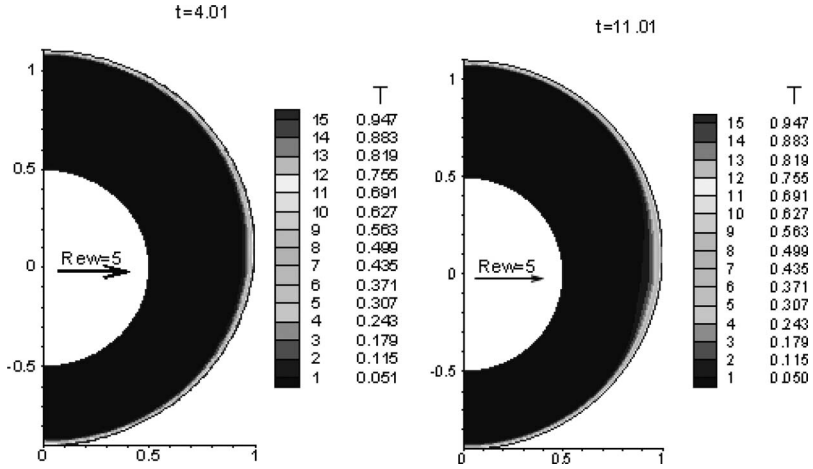

Fig. 14 Contours of T for Re=1000, $Re_w=5$, Pr=10, $\Omega_{io}=2\sin(\pi t/2)$, and $e=0.1$

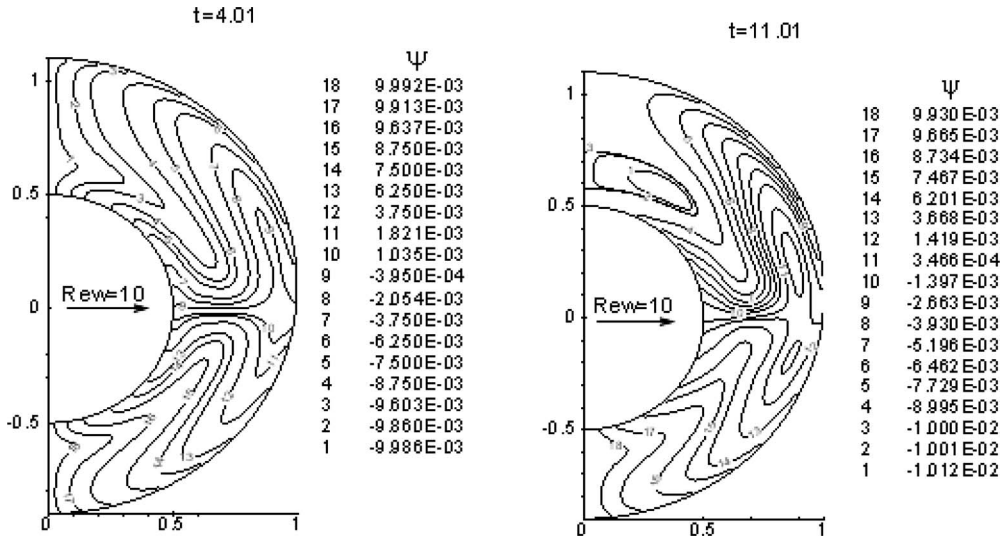

Fig. 15 Contours of ψ for Re=1000, Re_w=10, Ω_{io}=2 sin($\pi t/2$), and e=0.1

in this case, it is seen that the eddies near the outer sphere (in the vicinity of the equator) have more effects on the temperature field as these eddies prevent heat convection.

In the case Re_w=10 and t=4.01 (Fig. 15(*a*)), the eddies are nearly eliminated in the entire flow field. In this case, blowing helps the Coriolis forces to remove the eddies in the flow field. On the contrary, at t=11.01, Fig. 15(*b*), because the inner sphere rotates counter to the outer sphere (the inner sphere angular velocity is Ω_{io}=−1.998) the effects of Coriolis forces are against the blowing effects. In comparison with Fig. 15(*a*) the eddies have not been eliminated, although compared with Fig. 13(*b*), eddies are smaller (because of larger the values of Re_w). As a result, a change in the value and direction of rotation of the spheres and or the rate of blowing/suction can be used to regulate the flow field and therefore the rate of the heat transfer. The contours of T are shown in Fig. 16.

In Figs. 17–20 the contours of ψ and T are presented for the sinusoidal angular velocities and suction cases. Looking at their streamlines shows that eddies are created only in the vicinity of the poles. It is obvious that the size of the eddies and the distances between the stagnation points decrease with increasing suction rate.

Figures 21 and 22 present the flow field and heat transfer results for sinusoidal and exponential inner angular velocities for the case of concentric spheres (e=0). As it is observed from Fig. 21(*a*), in this case (Re_w=5) two stagnation points exist on the streamlines at the poles and also two stagnation points are at the equator. Streamlines for Re_w=10 have been drawn in Fig. 22(*a*) and it can be seen that there are no eddies in the flow field in this case.

The dimensionless viscous torque at any radius r for the case of eccentric spheres in general is

$$T_\mu = \frac{3}{4}\int_0^\pi \tau_{r\phi} \cdot r^3 \cdot \sin^2\theta \, d\theta \tag{9}$$

where the dimensionless shear stress $\tau_{r\phi}$ is

$$\tau_{r\phi} = -r\frac{\partial}{\partial r}\left(\frac{v_\phi}{r}\right) \tag{10}$$

Using the above definitions, variations of the viscous torques at the inner sphere $T_{\mu,i}$ and at the outer sphere $T_{\mu,o}$ with respect to time are presented in Figs. 23 and 24.

Tables 1 and 2 compare the results of the presented work with the analytical and numerical results of Ref. [18]. From these tables, suction decreases the thickness of the boundary layer of the inner sphere and, corresponding to this change, the coefficient of friction and therefore viscous torques on this sphere are increased.

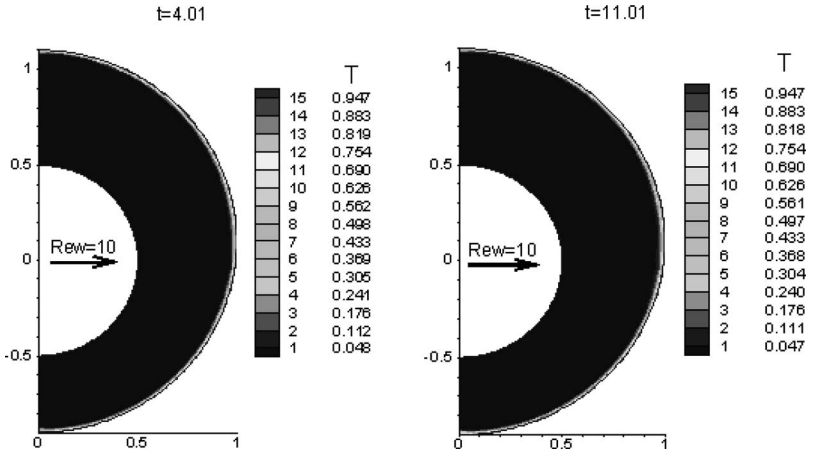

Fig. 16 Contours of T for Re=1000, Re_w=10, Pr=10, Ω_{io}=2 sin($\pi t/2$), and e =0.1

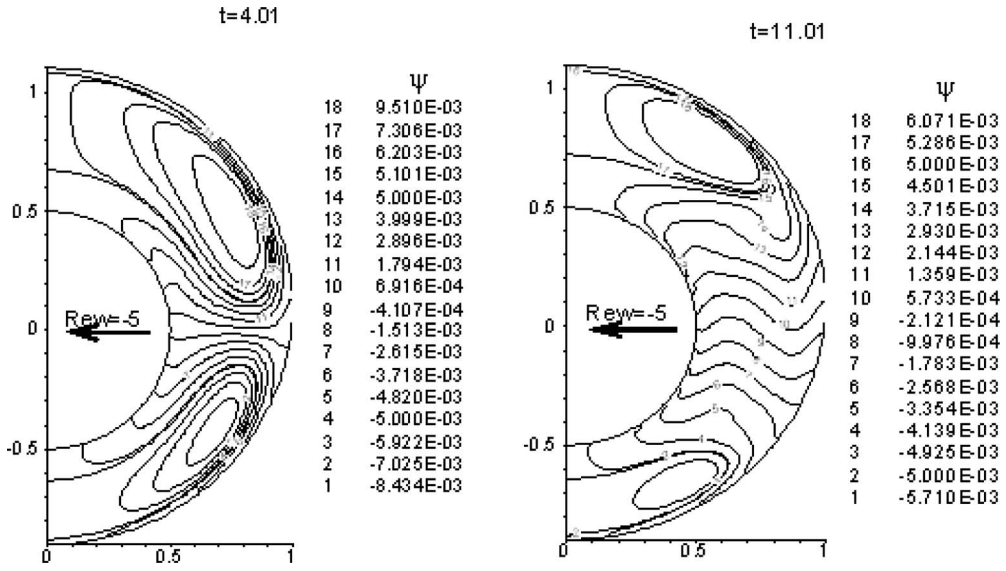

Fig. 17 Contours of ψ for Re=1000, Re_w=−5, Ω_{io}=2 sin($\pi t/2$), and e=0.1

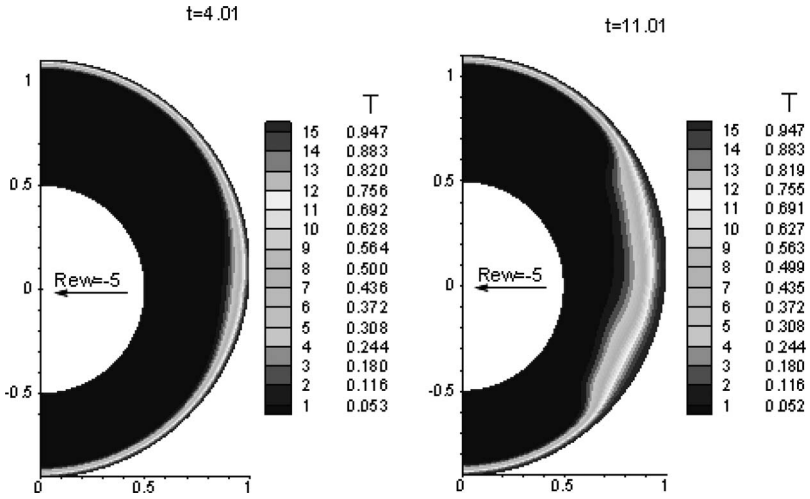

Fig. 18 Contours of T for Re=1000, Re_w=−5, Pr=10, Ω_{io}=2 sin($\pi t/2$), and e =0.1

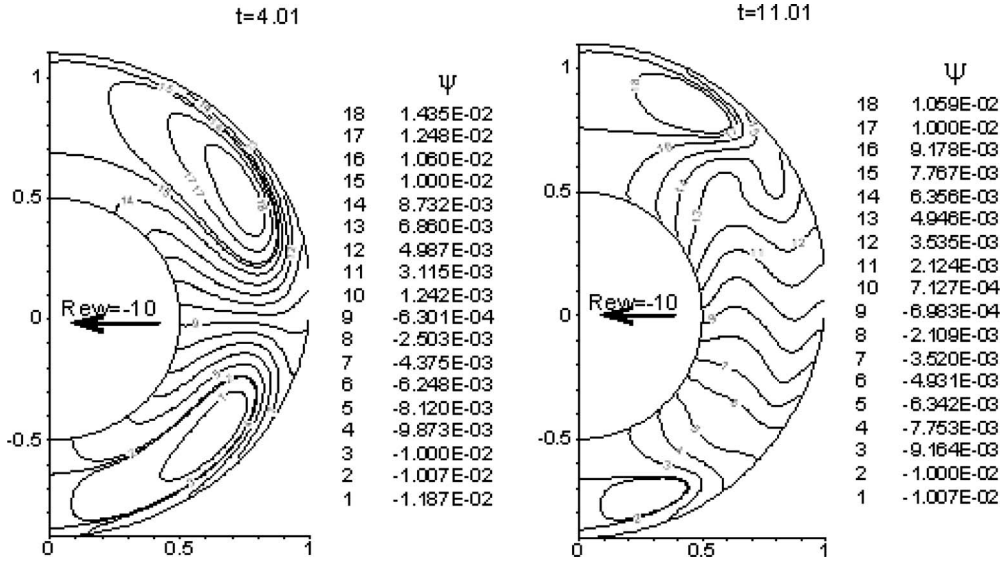

Fig. 19 Contours of ψ for Re=1000, Re_w=−10, Ω_{io}=2 sin($\pi t/2$), and e=0.1

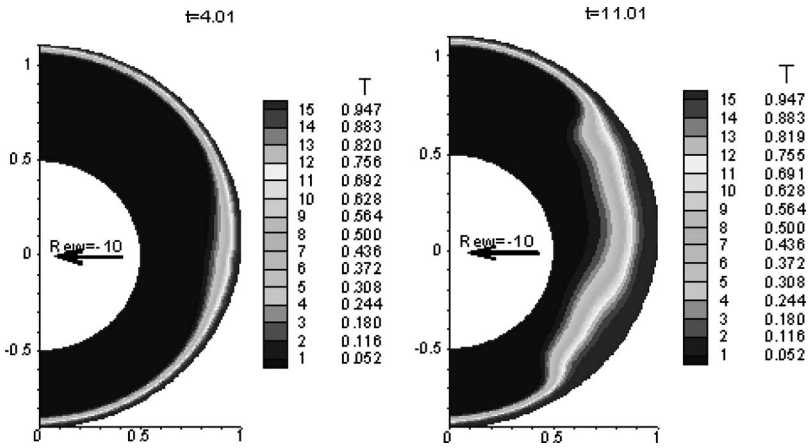

Fig. 20 Contours of T for Re=1000, Re_w=−10, Pr=10, Ω_{io}=2 sin($\pi t/2$), and e =0.1

The effect of suction on the outer sphere is that the boundary-layer thickness is increased and therefore the coefficient of friction and viscous torques are decreased.

Figure 23 shows the variation of $T_{\mu,i}$ with respect to time for Re=1000, Ω_{io}=2 sin($\pi t/2$), and e=0.1; it is seen that because the angular velocities of the inner sphere are sinusoidal the viscous torque is sinusoidal, too. Also it is observed that an increase in value of blowing decreases the average viscous torque.

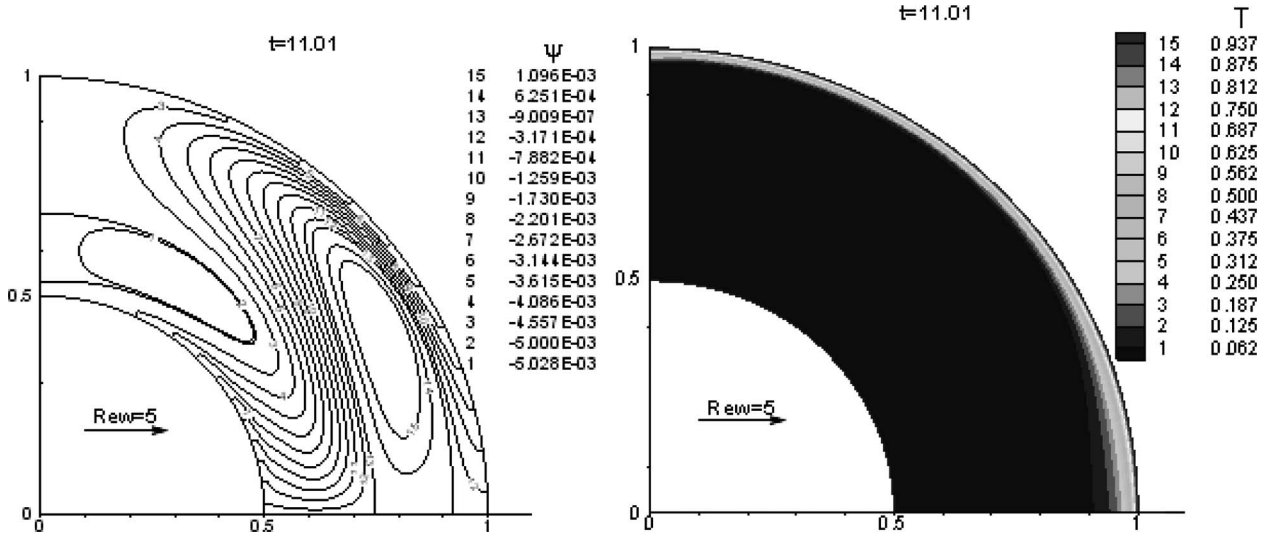

Fig. 21 Flow and heat transfer for Re=1000, Pr=10, Re_w=5, Ω_{io}=2 sin($\pi t/2$), and e=0

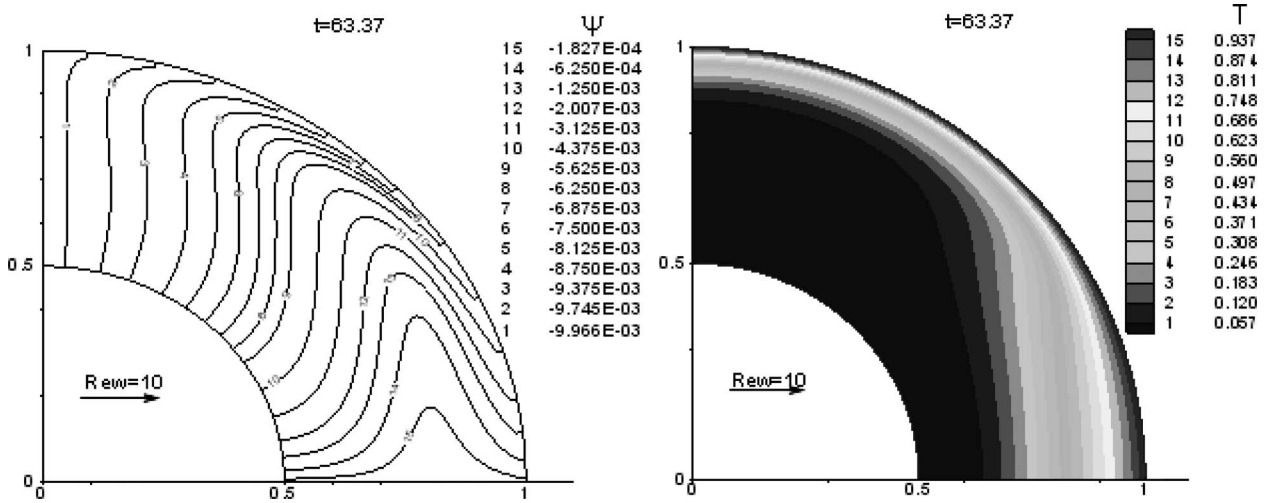

Fig. 22 Flow and heat transfer for Re=1000, Re_w=10, Pr=1, Ω_{io}=−exp(1−t), and e=0

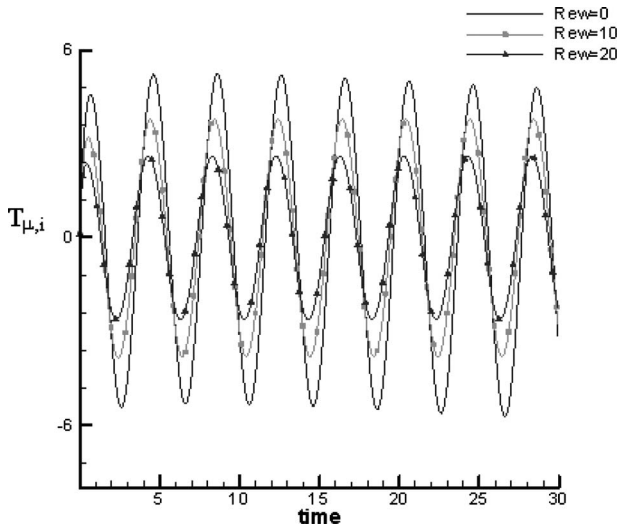

Fig. 23 Viscous torques at the inner sphere for Re=1000, Ω_{io} =2 sin(πt/2), and e=0.1

Table 3 shows that the effect of eccentricity is not considerable on viscous torque on the outer sphere and its effect on inner sphere is nearly zero.

Finally, the effect of Eckert number on heat transfer has been presented in Figs. 25 and 26. As can be seen from Fig. 25(*b*) the temperature field is over a wider area than Case (a) because of viscous dissipation, which plays the role of a source of heat. The effects of viscous dissipations are more visible in the vicinity of the equator because in this region the velocity gradients are longer. Also, the effect of Prandtl number on temperature field can be seen by comparing Figs. 18(*b*) and 25(*a*). A lower Prandtl number leads to more diffusions of heat.

Figure 26 is presented for the same conditions as in Fig. 20 except for Re_w=5. As can be seen in this case as well, the heat diffusion caused by viscous dissipation effects is more visible in the vicinity of the equator.

5 Conclusions

In this paper, the effects of transpiration on flow and heat transfer in an annulus between two rotating spheres (concentric and

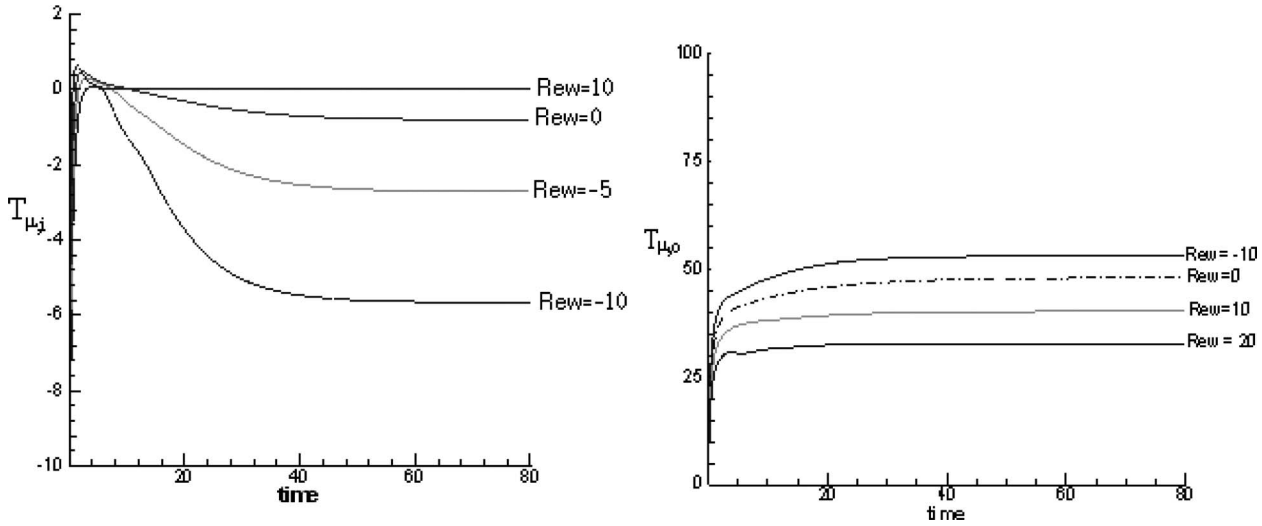

Fig. 24 Viscous torques at the inner and outer spheres for Re=1000, Ω_{io}=−exp(1−t), and e=0.05

Table 1 Viscous torques for Re=50, Ω_{oi}=0 for different values of blowing and its comparison with Ref. [18]

	$T_{\mu,i}$			$T_{\mu,o}$		
Case	Presented (T^*_μ Re)	Ref. 18 analytical	Ref. 18 numerical	Presented (T^*_μ Re)	Ref. 18 analytical	Ref. 18 numerical
Re_w=0	199.21	198.114	204.411	204.640	198.114	205.474
Re_w=1	186.794	187.102	192.929	243.826	237.102	243.177
Re_w=3	166.311	173.848	173.815	324.892	323.848	323.146
Re_w=5	150.987	169.739	158.578	409.619	419.739	407.537

Table 2 Viscous torques for Re=50, Ω_{oi}=0 for different values of suction and its comparison with Ref. [18]

	$T_{\mu,i}$			$T_{\mu,o}$		
Case	Presented (T^*_μ Re)	Ref. 18 analytical	Ref. 18 numerical	Presented (T^*_μ Re)	Ref. 18 analytical	Ref. 18 numerical
Re_w=0	199.21	198.114	204.411	204.640	198.114	205.474
Re_w=−1	214.885	212.558	217.593	169.269	162.558	169.805
Re_w=−3	254.80	253.275	251.177	106.164	103.275	107.252
Re_w=−5	310.688	312.311	298.178	59.896	62.311	60.168

Table 3 Re=1000, Re_w=−10, and Ω_{io}=−exp(1−t)

Eccentricity	$e=0$	$e=0.1$
$T_{\mu,o}$	53.293	53.020

eccentric) have been studied when the spheres have time-dependent prescribed values of angular velocities. The results have been presented for various values of blowing or suction Reynolds number, which indicates the strength of transpiration. Results show that increasing values of blowing or suction can be used to remove the eddies created in the flow field. Eliminating these eddies result in more heat to transfer. Eddies created in the upper and lower poles in eccentric case become smaller and larger, respectively, with decreasing the value of eccentricity and therefore the distance between two stagnation points on the upper pole decreases while in the lower pole the effect is opposite and these eddies obviously have equal sizes in the concentric case. With increasing blowing or suction the eddies are removed faster in the lower hemisphere due to more Coriolis forces.

Temperature field results show how the blowing and suction can be used to regulate the rate of heat transfer. In eccentric case, the diffusion of heat is more where the distance between two spheres is less. Results show that viscous dissipation effects appear near the equator because of higher velocities gradients causing more heat diffusions in this region. Finally, the effects of blowing and suction and also the eccentricity on viscous torques are studied. It is seen that the effects of the eccentricity on viscous torque are not substantial while blowing or suction has considerable effects on viscous torques.

Nomenclature

- Cp = specific heat at constant pressure
- D = substantial derivative
- E = nondimensional eccentricity
- Ek = Eckert number=$[\nu\omega_o/c_p(T_o-T_i)]$
- k = fluid conductivity
- Pe = Peclet number=υ/α
- r,θ,ϕ = spherical coordinates
- r_o = reference value for radius
- R_o' = characteristic radius of the outer sphere
- R_i = inner sphere radius
- R_o = outer sphere radius
- R_{io} = $=R_i/R_o$
- Re = Reynolds number=$(\omega_o r_o^2/\nu)$
- Re_w = blowing/suction Reynolds number=$(\upsilon_{r_o} r_o/\nu)$
- T = temperature
- T_i = inner sphere surface temperature
- T_o = outer sphere surface temperature
- t = time
- $\upsilon_r,\upsilon_\phi,\upsilon_\phi$ = velocity components

Greek

- α = thermal diffusivity
- υ = kinematic viscosity

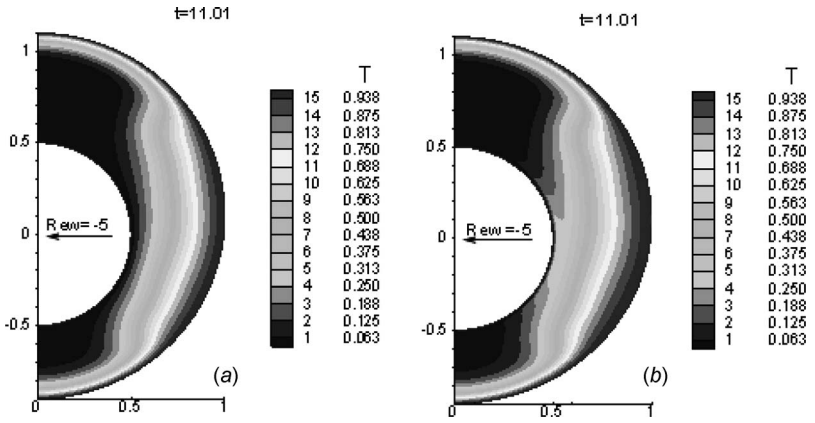

Fig. 25 Effect of viscous dissipation on temperature field for Re=1000, Re_w=−5, Pr=1, Ω_{io}=2 sin($\pi t/2$), and e=0.1: (*a*) Ek=0 and (*b*) Ek=0.001

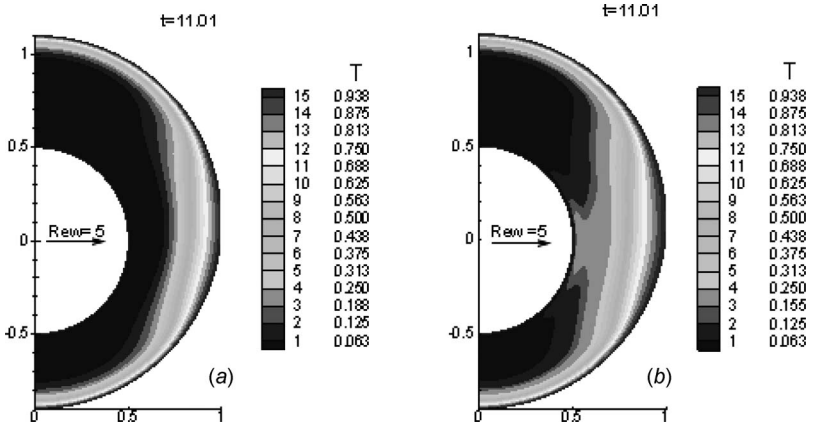

Fig. 26 Effect of viscous dissipation on temperature field for Re=1000, Re_w=5, Pr=10, Ω_{io}=2 sin($\pi t/2$), e=0.1: (*a*) Ek=0 and (*b*) Ek=0.001

ψ = stream function
Ω = momentum function
Ω_i = inner sphere angular velocity
Ω_o = outer sphere angular velocity
Ω_{oi} = Ω_i/Ω_o(in this case v_{R_o}, R_o, Ω_o are reference)
Ω_{oi} = $=\Omega_o/\Omega_i$ (in this case v_{R_i}, R_i, Ω_i are reference)
ω_o = reference value for angular velocity

References

[1] Howarth, L., 1951, "Note on Boundary Layer on a Rotating Sphere," Philos. Mag., **7**(42), pp. 1308–1311.
[2] Proudman, I., 1956, "The Almost-Rigid Rotation of Viscous Fluid Between Concentric Spheres," J. Fluid Mech., **1**, pp. 505–516.
[3] Lord, R. G., and Bowden, F. P., 1963, "Boundary Layer on a Rotating Sphere," Proc. R. Soc. London, Ser. A, **271**, pp. 143–146.
[4] Fox, J., 1964, "Singular Perturbation of Viscous Fluid Between Spheres," NASA, Report No. TN D-2491.
[5] Greenspan, H. P., 1964, "Axially Symmetric Motion of a Rotating Fluid in a Spherical Annulus," J. Fluid Mech., **20**, pp. 673–677.
[6] Carrier, G. F., 1966, "Some Effects of Stratification and Geometry in Rotating Fluids," J. Fluid Mech., **24**, pp. 641–659.
[7] Stewartson, K., 1966, "On Almost Rigid Rotations. Part 2," J. Fluid Mech., **26**, pp. 131–144.
[8] Pearson, C., 1967, "A Numerical Study of the Time-Dependent Viscous Flow Between Two Rotating Spheres," J. Fluid Mech., **28**(2), pp. 323–336.
[9] Munson, B. R., and Joseph, D. D., 1971, "Viscous Incompressible Flow Between Concentric Rotating Spheres, Part I: Basic Flow," J. Fluid Mech., **49**, pp. 289–303.
[10] Douglass, R. W., Munson, B. R., and Shaughnessy, E. J., 1978, "Thermal Convection in Rotating Spherical Annuli—1. Forced Convection," Int. J. Heat Mass Transfer, **21**, pp. 1543–1553.
[11] Munson, B. R., and Douglass, R. W., 1979, "Viscous Flow in Oscillatory Spherical Annuli," Phys. Fluids, **22**(2), pp. 205–208.
[12] Gagliardi, J. C., Nigro, N. J., Elkouh, A. F., and Yang, J. K., 1990, "Study of the Axially Symmetric Motion of an Incompressible Viscous Fluid Between Two Concentric Rotating Spheres," J. Eng. Math., **24**, pp. 1–23.
[13] Yang, J. K., Nigro, N. J., and Elkouh, A. F., 1989, "Numerical Study of the Axially Symmetric Motion of an Incompressible Viscous Fluid in an Annulus Between Two Concentric Rotating Spheres," Int. J. Numer. Methods Fluids, **9**, pp. 689–712.
[14] Ni, W., and Nigro, N. J., 1994, "Finite Element Analysis of the Axially Symmetric Motion of an Incompressible Viscous Fluid in a Spherical Annulus," Int. J. Numer. Methods Fluids, **19**, pp. 207–236.
[15] Jabari Moghadam, A., and Rahimi, A. B., 2008, "A Numerical Study of Flow and Heat Transfer Between Two Rotating Spheres With Time-Dependent Angular Velocities," ASME J. Heat Transfer, **130**, p. 071703.
[16] Jabari Moghadam, A., and Rahimi, A. B., 2009, "Similarity Solution in Study of Flow and Heat Transfer Between Two Rotating Spheres With Constant Angular Velocities," International Journal of Science and Technology, SCIENTIA IRANCA, **16**(4), pp. 354–362.
[17] Gulwadi, S. D., and Elkouh, A. F., 1994, "Effects of Transpiration on Free Convection in an Annulus Between Concentric Porous Spheres," J. Eng. Math., **28**, pp. 483–499.
[18] Gulwadi, S. D., Elkouh, A. F., and Jan, T. C., 1993, "Laminar Flow in an Annulus Between Two Concentric Rotating Porous Spheres," Acta Mech., **97**, pp. 215–228.
[19] Press, W. H., Flannery, B. P., Teukolsky, S. A., and Vetterling, W. T., 1997, *Numerical Recipes, the Art of Scientific Computing*, Cambridge University Press, Cambridge.